Supplemental Material
Imaging topological defects in a non-collinear antiferromagnet

Aurore Finco,[1] Angela Haykal,[1] Stéphane Fusil,[2] Pawan Kumar,[1]
Pauline Dufour,[2] Anne Forget,[3] Dorothée Colson,[3] Jean-Yves Chauleau,[3]
Michel Viret,[3] Nicolas Jaouen,[4] Vincent Garcia,[2] and Vincent Jacques[1]

[1]*Laboratoire Charles Coulomb, CNRS, Université de Montpellier, 34095 Montpellier, France*

[2]*Unité Mixte de Physique, CNRS, Thales, Université Paris-Saclay, 91767 Palaiseau, France*

[3]*SPEC, CEA, CNRS, Université Paris-Saclay, 91191 Gif sur Yvette, France*

[4]*Synchrotron SOLEIL, 91192 Gif-sur-Yvette, France*

I. ESTIMATION OF m_{DM} FROM A QUANTITATIVE FIELD MEASUREMENT

A. Calibration of the NV-to-sample distance

The first step in the quantitative analysis is to determine the distance d_{NV} between the NV center and the sample surface. To achieve this, we follow the calibration procedure described in ref. [1]. First, we measure the direction of the NV center quantization axis by recording the ESR frequency as a function of the orientation of a calibrated magnetic field. We obtain the polar angle $\theta_{\mathrm{NV}} = 120°$ and the azimuthal angle $\varphi_{\mathrm{NV}} = 5°$. Then we measure a magnetic stray field profile across a well-characterized ferromagnetic stripe with perpendicular magnetic anisotropy. Using the analytical expression of the stray field generated by the edges and our knowledge of the NV center orientation, we fit the experimental profile, as shown in Fig S1, and extract the value of $d_{\mathrm{NV}} = 60 \pm 1\,\mathrm{nm}$.

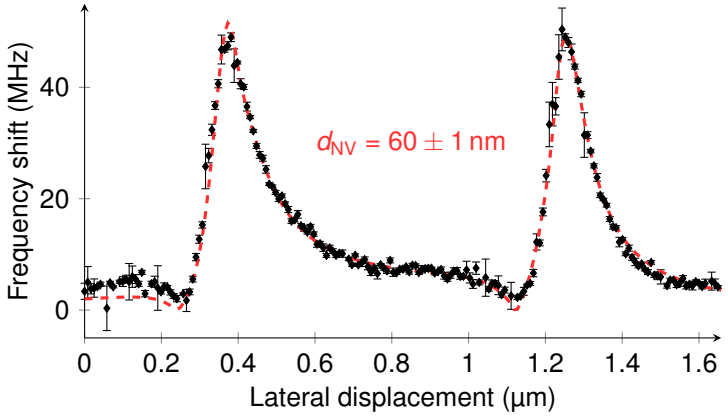

FIG. S1. Magnetic stray field profile measured across a ferromagnetic stripe, fitted analytically in order to extract the value of d_{NV}.

B. Measurement of the stray field from the magnetic texture

Next, we measure the stray field produced by the magnetic texture with a scanning-NV magnetometer operating under ambient conditions. A commercial diamond tip hosting a single NV defect at its apex (Qnami, Quantilever MX) is integrated into an atomic force microscope and scanned in close proximity of the bulk $BiFeO_3$ crystal surface. At each point of the scan, a quantitative magnetic field measurement is obtained by monitoring the Zeeman shift of the NV defect electron spin sublevels through optical detection of the magnetic resonance. Note that the in dual-iso-B mode used in the main text, we only measure the difference of photoluminescence intensity for two fixed RF frequencies applied consecutively at each point of the scan. This measurement mode provides a qualitative insight on the variations of the magnetic stray field.

The obtained quantitative field map above a domain in which the cyloid propagates along $\mathbf{k_3}$ is presented in Fig. S2 and shows a magnetic field modulation with a typical amplitude in the range of 100 µT. A line profile was extracted along the dashed line and fitted using the analytical expression derived in the next section, using the values of the parameters θ_{NV}, φ_{NV} and d_{NV} resulting from the calibration procedure described above. This analysis leads to $m_{\mathrm{DM}} = 0.09 \pm 0.03\ \mu_{\mathrm{B}}$.

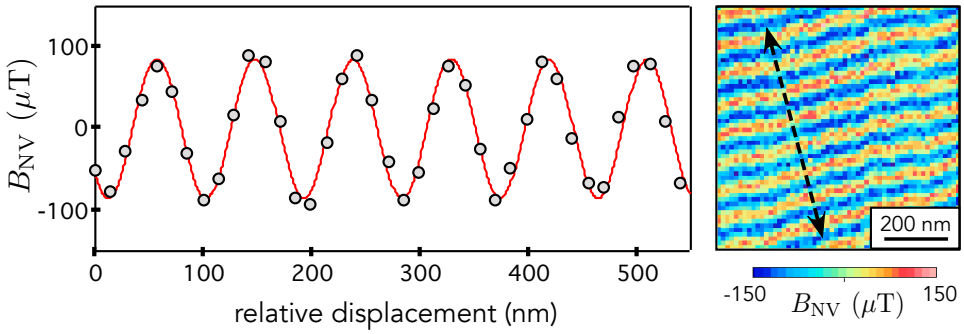

FIG. S2. Quantitative measurement of the stray field produced by the $\mathbf{k_3}$ variant of the cycloid. The line profile is extracted along the indicated dashed line and fitted using the analytical expression derived in the next section.

C. Analytical expression of the stray field produced by the $\mathbf{k_3}$ variant of the cycloid

We consider a $BiFeO_3$ bulk crystal with a (001) surface, and the ferroelectric polarization $\mathbf{P}$ along the [111] direction. We want to compute the stray field $\mathbf{B}$ generated by the magnetic texture in a domain where the cycloid is propagating along $\mathbf{k_3}$, which is parallel to the $[0\bar{1}1]$ direction. In the cyloid itself, the antiferromagnetic ordering results in a perfect compensation of the magnetic moments. Therefore, the only component of the magnetic texture contributing to the stray field is the spin density wave. We describe it as:

$$\mathbf{M}_{\mathrm{SDW}}(\mathbf{r}) = \frac{m_{\mathrm{DM}}}{a^3\sqrt{6}} \cos(\mathbf{k_3} \cdot \mathbf{r})(-2\mathbf{e}_x + \mathbf{e}_y + \mathbf{e}_z) \tag{1}$$

with $a = 3.96\,\text{Å}$ the $BiFeO_3$ unit cell size. It leads to:

$$\begin{cases} M_x = -\dfrac{2m_{\text{DM}}}{a^3\sqrt{6}} \cos\left(\dfrac{k}{\sqrt{2}}(y-z)\right) \\ M_y = \dfrac{m_{\text{DM}}}{a^3\sqrt{6}} \cos\left(\dfrac{k}{\sqrt{2}}(y-z)\right) \\ M_z = \dfrac{m_{\text{DM}}}{a^3\sqrt{6}} \cos\left(\dfrac{k}{\sqrt{2}}(y-z)\right) \end{cases} \tag{2}$$

We introduce the potential Φ such that $\mathbf{B} = -\boldsymbol{\nabla}\Phi$. This potential can be expressed as:

$$\Phi(\mathbf{r}) = -\frac{\mu_0}{4\pi} \int \mathbf{M}(\mathbf{r}') \cdot \boldsymbol{\nabla}' \frac{1}{|\mathbf{r}-\mathbf{r}'|} \mathrm{d}\mathbf{r}' \tag{3}$$

Eq.(3) is a convolution, so we can easily compute Φ in Fourier space:

$$\Phi = \mathcal{F}^{-1}\left[\mathcal{F}[\mathbf{M}]\ \mathcal{F}\left[\boldsymbol{\nabla}\left(\frac{1}{r}\right)\right]\right] \tag{4}$$

Note that we have [2]:

$$\mathcal{F}\left[\frac{1}{r}\right](q) = 2\pi \frac{e^{-|q|(z-z')}}{|q|} \quad \text{for} \quad |q| \neq 0 \quad \text{and} \quad z' < z. \tag{5}$$

For a single $BiFeO_3$ layer of thickness a, we get:

$$\begin{aligned} \Phi = -\frac{\mu_0}{4\pi} \int_{z'=-a/2}^{z'=a/2} \Bigg(\iint_{-\infty}^{\infty} \Big[& iq_x \mathcal{F}(M_x) \mathcal{F}\left(\frac{1}{r}\right) + iq_y \mathcal{F}(M_y) \mathcal{F}\left(\frac{1}{r}\right) \\ & -|q| \mathcal{F}(M_z) \mathcal{F}\left(\frac{1}{r}\right) \Big] e^{ixq_x + iyq_y}\, \mathrm{d}q_x\, \mathrm{d}q_y \Bigg) \mathrm{d}z' \end{aligned} \tag{6}$$

Rewriting Eq.(6) as $\Phi = -\dfrac{\mu_0}{4\pi} \displaystyle\int_{z'=-a/2}^{z'=a/2} (I + II + III)\, \mathrm{d}z'$, we compute each term separately.

$$\begin{aligned} I &= \iint_{-\infty}^{\infty} iq_x \mathcal{F}(M_x)\ \mathcal{F}\left(\frac{1}{r}\right)\ e^{ixq_x} e^{iyq_y}\, \mathrm{d}q_x\, \mathrm{d}q_y \\ I &= \left(\int_{-\infty}^{\infty} iq_x \delta(q_x) e^{ixq_x}\, \mathrm{d}q_x \right) \\ &\quad \times \left(\int_{-\infty}^{\infty} \frac{-2m_{\text{DM}}}{a^3\sqrt{6}} \left[e^{-ikz/\sqrt{2}}\ \delta\left(\frac{k}{\sqrt{2}} - q_y\right) + e^{ikz/\sqrt{2}}\ \delta\left(\frac{k}{\sqrt{2}} + q_y\right) \right] 2\pi \frac{e^{-|q|(z-z')}}{|q|}) e^{iyq_y}\, \mathrm{d}q_y \right) \\ I &= 0 \end{aligned} \tag{7}$$

$$II = \iint_{-\infty}^{\infty} iq_y \mathcal{F}(M_y)\ \mathcal{F}\left(\frac{1}{r}\right)\ e^{ixq_x} e^{iyq_y}\,\mathrm{d}q_x\,\mathrm{d}q_y$$

$$II = \iint_{-\infty}^{\infty} iq_y \frac{m_{\mathrm{DM}}}{a^3\sqrt{6}}\ \frac{\delta(q_x)}{2}\left[e^{-ikz/\sqrt{2}}\ \delta\left(\frac{k}{\sqrt{2}} - q_y\right) + e^{ikz/\sqrt{2}}\ \delta\left(\frac{k}{\sqrt{2}} + q_y\right)\right] \times 2\pi \frac{e^{-|q|(z-z')}}{|q|}\ e^{ixq_x} e^{iyq_y}\,\mathrm{d}q_x\,\mathrm{d}q_y$$

$$II = -2\pi \frac{k}{\sqrt{2}} \frac{m_{\mathrm{DM}}}{a^3\sqrt{6}} \frac{e^{-k(z-z')/\sqrt{2}}}{\frac{k}{\sqrt{2}}} \frac{1}{2i}\left[e^{-ikz/\sqrt{2}} e^{iky/\sqrt{2}} - e^{ikz/\sqrt{2}} e^{-iky/\sqrt{2}}\right]$$

$$II = -2\pi \frac{m_{\mathrm{DM}}}{a^3\sqrt{6}} e^{-k(z-z')/\sqrt{2}} \sin\left(\frac{k}{\sqrt{2}}(y-z)\right) \tag{8}$$

$$III = \iint_{-\infty}^{\infty} -|q|\ \mathcal{F}(M_z)\ \mathcal{F}\left(\frac{1}{r}\right)\ \ e^{ixq_x} e^{iyq_y}\,\mathrm{d}q_x\,\mathrm{d}q_y$$

$$III = \iint_{-\infty}^{\infty} -|q| \frac{m_{\mathrm{DM}}}{a^3\sqrt{6}}\ \frac{\delta(q_x)}{2}\left[e^{-ikz/\sqrt{2}}\ \delta\left(\frac{k}{\sqrt{2}} - q_y\right) + e^{ikz/\sqrt{2}}\ \delta\left(\frac{k}{\sqrt{2}} + q_y\right)\right] \times 2\pi \frac{e^{-|q|(z-z')}}{|q|}\ e^{ixq_x} e^{iyq_y}\,\mathrm{d}q_x\,\mathrm{d}q_y$$

$$III = -\frac{m_{\mathrm{DM}}}{a^3\sqrt{6}} 2\pi e^{-k(z-z')} \frac{1}{2}\left[e^{-ikz/\sqrt{2}} e^{iky/\sqrt{2}} + e^{ikz/\sqrt{2}} e^{-iky/\sqrt{2}}\right]$$

$$III = -2\pi \frac{m_{\mathrm{DM}}}{a^3\sqrt{6}} e^{-k(z-z')/\sqrt{2}} \cos\left(\frac{k}{\sqrt{2}}(y-z)\right) \tag{9}$$

$$\tag{10}$$

We bring everything together and we have, still for a $BiFeO_3$ single layer:

$$\Phi = \frac{\mu_0 m_{\mathrm{DM}}}{\sqrt{3}a^3} \frac{e^{-kz/\sqrt{2}}}{k} \sinh\left(\frac{ka}{2\sqrt{2}}\right)\left[\cos\left(\frac{k}{\sqrt{2}}(y-z)\right) + \sin\left(\frac{k}{\sqrt{2}}(y-z)\right)\right] \tag{11}$$

The corresponding stray field $\mathbf{B} = -\boldsymbol{\nabla}\Phi$ is:

$$\begin{cases} B_x = 0 \\ B_y = -\dfrac{\mu_0\ m_{\mathrm{DM}}}{\sqrt{6}a^3} e^{-kz/\sqrt{2}} \sinh\left(\dfrac{ka}{2\sqrt{2}}\right)\left[\cos\left(\dfrac{k}{\sqrt{2}}(y-z)\right) - \sin\left(\dfrac{k}{\sqrt{2}}(y-z)\right)\right] \\ B_z = \sqrt{\dfrac{2}{3}} \dfrac{\mu_0\ m_{\mathrm{DM}}}{a^3} e^{-kz/\sqrt{2}} \sinh\left(\dfrac{ka}{2\sqrt{2}}\right) \cos\left(\dfrac{k}{\sqrt{2}}(y-z)\right) \end{cases} \tag{12}$$

To get the value of the stray field for the whole crystal of thickness t constituted of $N = \frac{t}{a}$ layers, we have to sum these terms with $z \to z + ja$ ($j \in [0, N-1]$). Defining:

$$\mathcal{S} = \sum_{j=0}^{N-1} e^{-k(z+ja)/\sqrt{2}} e^{\frac{ik}{\sqrt{2}}(y-z+ja)} = e^{-kz/\sqrt{2}} e^{ik(y-z)/\sqrt{2}}\ \frac{1 - e^{-kt(1+i)/\sqrt{2}}}{1 - e^{-ka(1+i)/\sqrt{2}}} \tag{13}$$

and

$$\mathcal{A} = \frac{\mu_0 m_{\mathrm{DM}}}{\sqrt{3}a^3} \sinh\left(\frac{ka}{2\sqrt{2}}\right) \tag{14}$$

we reach the final expression for the stray field generated by the spin density wave in a domain where the cycloid propagates along $\mathbf{k_3}$ in a $BiFeO_3$ crystal of thickness t:

$$\begin{cases} B_x = 0 \\ B_y = -\dfrac{\mathcal{A}}{\sqrt{2}} \left(\mathrm{Re}\{\mathcal{S}\} - \mathrm{Im}\{\mathcal{S}\}\right) \\ B_z = \sqrt{2}\mathcal{A}\,\mathrm{Re}\{\mathcal{S}\} \end{cases} \tag{15}$$

II. WAVEVECTOR ELLIPSE

If we assume that the wavevector $\mathbf{k}$ of the cycloid rotates but stays in the (111) plane and that the period λ_b of the cycloid does not depend on the direction of $\mathbf{k}$, the ensemble of all the possible cycloid wavevectors describes a circle in the (111) plane. Both with NV magnetometry and REXS, we probe the surface plane, which is a (001) plane of the bulk $BiFeO_3$ crystal. The projection of the circle of radius $k = \frac{2\pi}{\lambda_b}$ in (111) plane onto the (001) is the ellipse depicted in Fig. S3. Its polar equation, with $\theta = 0°$ aligned along $\mathbf{k_1}$ is:

$$r(\theta) = \frac{2\pi}{\lambda_b} \frac{1}{\sqrt{3 - 2\cos^2\theta}} \tag{16}$$

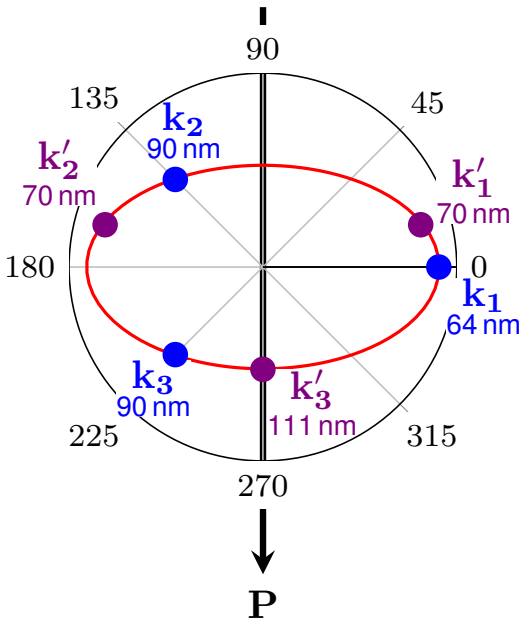

FIG. S3. Sketch of the ellipse corresponding to the projection on the (001) plane of a circle of radius $k = \frac{2\pi}{\lambda_b}$ in the (111) plane. The propagation directions corresponding to the cycloid type I ($\mathbf{k_1}$, $\mathbf{k_2}$ and $\mathbf{k_3}$) and to the cycloid type II ($\mathbf{k'_1}$, $\mathbf{k'_2}$ and $\mathbf{k'_3}$) are indicated, as well as the corresponding projected period.

III. SIZE OF THE TOPOLOGICAL DEFECTS

One can roughly estimate the typical size of the topological defects by enclosing them in circles outside which the curvature of the lamellar texture is not influenced anymore by their presence. We find that circles of radius $2\lambda_b \simeq 130\,\text{nm}$ appear to have an appropriate size, as shown in Fig. S4.

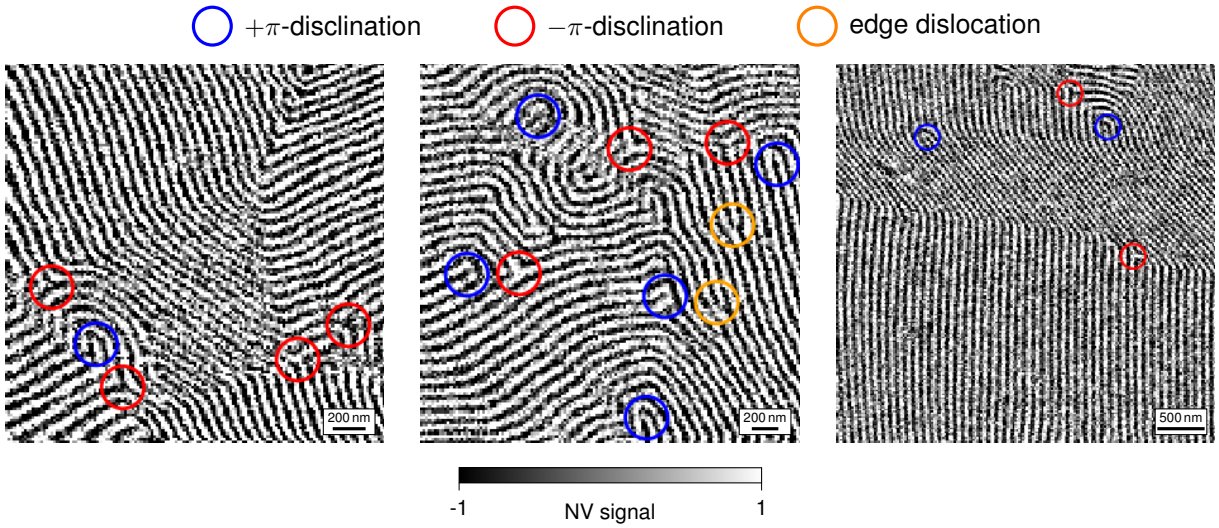

FIG. S4. NV images of the cycloidal texture in bulk $BiFeO_3$, with circles of radius 130 nm enclosing the topological defects.

[1] T. Hingant, J.-P. Tetienne, L. J. Martínez, K. Garcia, D. Ravelosona, J.-F. Roch, and V. Jacques, Phys. Rev. Applied **4**, 014003 (2015).

[2] R. J. Blakely, *Potential theory in gravity and magnetic applications* (Cambridge University Press, 1995).